

Modeling financial distress propagation on customer–supplier networks

Cite as: Chaos 31, 053119 (2021); doi: 10.1063/5.0041104

Submitted: 19 December 2020 · Accepted: 27 April 2021 ·

Published Online: 18 May 2021



View Online



Export Citation



CrossMark

Jordi Nin,^{1,a)} Bernat Salbanya,^{1,b)} Pablo Fleurquin,^{2,c)} Elena Tomás,^{3,d)} Alex Arenas,^{4,e)} and José J. Ramasco^{2,f)}

AFFILIATIONS

¹ESADE, Universitat Ramon Llull, 08034 Barcelona, Spain

²Instituto de Física Interdisciplinar y Sistemas Complejos (IFISC), CSIC-UIB, 07122 Palma de Mallorca, Spain

³Repsol Data & Analytics Hub, 28935 Madrid, Spain

⁴Departament Enginyeria Informàtica i Matemàtiques, Universitat Rovira i Virgili, 43007 Tarragona, Spain

^{a)}Electronic mail: jordi.nin@esade.edu

^{b)}Author to whom correspondence should be addressed: bernat.salbanya@esade.edu

^{c)}Electronic mail: pablo.fleurquin@gmail.com

^{d)}Electronic mail: elena.tomas@repsol.com

^{e)}Electronic mail: alexandre.arenas@urv.cat

^{f)}Electronic mail: jramasco@ifisc.uib-csic.es

ABSTRACT

Financial networks have been the object of intense quantitative analysis during the last few decades. Their structure and the dynamical processes on top of them are of utmost importance to understand the emergent collective behavior behind economic and financial crises. In this paper, we propose a stylized model to understand the “domino effect” of distress in client–supplier networks. We provide a theoretical analysis of the model, and we apply it to several synthetic networks and a real customer–supplier network, supplied by one of the largest banks in Europe. Besides, the proposed model allows us to investigate possible scenarios for the functioning of the financial distress propagation and to assess the economic health of the full network. The main novelty of this model is the combination of two stochastic terms: an additive noise, accounting by the capability of trading and paying obligations, and a multiplicative noise representing the variations of the market. Both parameters are crucial to determining the maximum default probability and the diffusion process characteristics.

Published under an exclusive license by AIP Publishing. <https://doi.org/10.1063/5.0041104>

Business interactions daily form a direct and weighted customer–supplier network whose structure has in-depth implications in its functioning. The financial distress of one company depends on the ability of their clients to fulfill their payments. Otherwise, a firm is not able to keep on working unless it applies for a loan. The recent financial crisis has prompted much new research on the interconnectedness of companies and the extent to which it contributes to systemic fragility. Here, we explore the interplay between network complexity and market stability in a deliberately simplified model for financial distress propagation.

I. INTRODUCTION

Network theory and non-linear systems have been widely used in economy and finance.^{1–4} In particular, the study of

customer–supplier networks is increasingly growing because of their fundamental role in the optimization of the production chain and the analysis of a systemic risk.^{5–8} Although companies select whom to trade with, they do not control whom the clients of their suppliers are.⁹ Consequently, instead of having a neat supply chain, suppliers and clients are all interrelated as entities of a large complex trading network.

Economic network properties have been studied at different scales, e.g., countries,¹⁰ industries,³ or stock exchange markets.¹¹ Interestingly, those networks showed a power-law degree distribution, implying the existence of hubs. Explanations for this phenomenon have been largely investigated in the network dynamics area as the “rich-gets-richer” effect by using different models.^{12,13} Beyond the distribution of connections, other characteristics such as the clustering level have been studied.¹⁴ A

complete review of empirical economic network models can be found at Ref. 15.

One of the main conclusions of these works is that the heterogeneity of network connectivity strongly affects the probability of observing a large scale effect, the most disquieting being the possibility of failure cascades,^{16–18} which increase the systemic risk and the fragility of financial and economic systems.^{19–22} A simple rule of thumb can be deduced from these works: the larger the average degree of the network, the larger the probability of observing a system-size cascade. Moreover, recent studies revealed significant correlations between local topological properties of a given node and its risk of default combined with business cycle correlations between communities. Such correlations make that firms with a similar risk profile are statistically more connected among themselves.^{23–25} Knowing this, the surge of financial distress in some companies in a real network, combined with the rapid spread of the uncertainty about its consequences, may lead to a significant increase in volatility, making the whole system more vulnerable to adverse economic events.^{26,27} Therefore, the analysis and forecasting of scenarios where the resilience of real financial networks is prone to contagion, as well as the circumstances under which it becomes systemic, have a paramount importance.^{28–31,38,39}

Several works have analyzed the dynamics of financial distress propagation using different models and networks.^{32–34} In particular, we focus our attention on Ref. 35, where an additive model of the economy was introduced. In this model, the time evolution is described by an equation capturing both exchanges between individuals and random speculative trading on a synthetic heterogeneous (power-law) network. The main conclusion of this work is that wealth tends to concentrate on a few agents following a “Pareto”-tail distribution. The authors drew this conclusion using a simple but effective equation where trading was introduced as two independent additive noises over time.

Following the intuition introduced in this paper,³⁵ our work formalizes a flexible and intuitive model for quantifying distress and default contagion in customer–supplier networks. Our proposed model incorporates any possible network information and a combination of additive and multiplicative noise interactions, representing the network economic activity and market volatility, respectively.

The model aims at quantifying the problem of distress propagation based on two stylized factors: the capability of companies to trade and the market uncertainty or volatility. Here, we understand trading as the company’s ability to collect and pay debts and volatility as an external factor affecting each company independently. After checking analytically that our model reaches a steady-state, we perform a set of experimental scenarios using synthetic network topologies. From them, it is possible to extract meaningful insights about how network topology affects distress propagation. Finally, we demonstrate our model’s applicability in a real customer–supplier network provided by a Spanish bank.

The rest of this paper is organized as follows. First, the theoretical basis for distress propagation is introduced in Sec. II, and in Secs. III and IV, we analyze the model from a numerical perspective. Then, in Sec. V, we discuss meaningful insights from several synthetic but realistic network structures. In Sec. VI, we validate our model in a real network provided by a large bank in Spain. This

paper concludes with a summary of our findings and an outline of future research.

II. FINANCIAL DISTRESS PROPAGATION MODEL

In accordance with Ref. 35, we assume that the liquidity of a company is a time-dependent variable elusive to direct quantification. However, it could be inferred through two elements: the market volatility and the money exchanged in the collection and payments network. On the one hand, volatility may affect companies’ payment capacity depending on their market exposure. On the other hand, its collection and payments structure and activation will be essential for it is the cause of the exposure of the company liquidity to its clients’ liquidity. There is an additional element, the liquidity ratio at time 0, which stands for the initial conditions of the company. The larger this ratio, the more resilient the company will be to external volatility and changes in its network. Once stated that the balance equations that infer the liquidity of a company can be extended to an interacting model, we call a *liquidity model*. Its mathematical formulation is as follows:

$$L_i(t+1) = L_i(t) (1 + \eta(0, \sigma)) + \sum_{j \in N_i} w_{ji} P(t) H(L_j(t) - w_{ji}) - \sum_{j \in N_i} w_{ij} P(t) H(L_i(t) - w_{ij}), \quad (1)$$

where $L_i(t)$ stands for the amount of money of node i at time t , which represents the available liquidity, and $\eta(0, \sigma)$ represents a Gaussian noise with mean μ equal to 0 and a standard deviation σ . Then, N_i stands for the set of neighbors for node i ; thus, w_{ji} and w_{ik} correspond to the weight of an edge from j to i and vice versa. $P(t)$ is a random variable that follows a Bernoulli distribution with probability p . Finally, $H(L_i(t) - w_{ij})$ represents a Heaviside step function that evaluates to 1 if the node i has enough money for doing the transfer and 0 otherwise.

The proposed model depends on three main parameters: $L_i(0)$, the liquidity at time $t = 0$; σ , which accounts for market volatility; and p , which accounts for the money exchange in the collection and payments network. Note that several L_i prescriptions are possible. Here, we consider that it corresponds to the ratio between the in-strength and out-strength of the node R_i . Other prescriptions do not affect the main message of this paper. The market volatility is supposed to follow a Gaussian distribution where μ and σ account for the mean and standard deviation. The volatility effect is proportional to the liquidity of the company and may affect in a positive or negative way; for this reason, we have considered the mean to be zero ($\mu = 0$). These impacts are the result of changes in the current scenario. The money exchange is controlled by a global parameter p ranging from 0 to 1. When $p = 1$, the network is fully activated, meaning that all money exchanges are taking place. When the network is not fully activated, p is the fraction of active payments.

III. ANALYSIS OF THE MODEL

The aforementioned discrete model allows us to simulate different scenarios. In this section, we focus on a very simple scenario

yet analytically tractable, consisting of a single company interacting with an external market. In this particular case, we can perform an analytical continuation of the discrete equations.

Keeping the same notation as above, the evolution of the liquidity of a single company could be written as a Langevin equation as

$$\frac{dL}{dt} = L \psi(t) + \eta(t) + c, \tag{2}$$

where c is a constant accounting for the unbalance between incoming and outgoing money flows and connects to R_s in the discrete model [$c = (R_s - 1) s_{out}$, where s_{out} is the initial total money output of the node], $\psi(t)$ and $\eta(t)$ are random noises with averages $\langle \eta \rangle = \langle \psi \rangle = 0$ and correlations

$$\begin{aligned} \langle \eta(t) \eta(t') \rangle &= \alpha^2 \delta(t - t'), \\ \langle \psi(t) \psi(t') \rangle &= \sigma^2 \delta(t - t'), \end{aligned} \tag{3}$$

where $\delta()$ is the Dirac delta and α and σ are related to other two parameters of our discrete model. In the case of σ , the identification is direct, while the variance of the binomial should be represented by α^2 , $p(1 - p) = \alpha^2$. Equation (2) must be considered in the Itô interpretation because the variable $L(t)$ and the noise $\psi(t)$ are independent when multiplied at time t .

Following Gardiner³⁶ and Toral,³⁷ one can write a Fokker-Planck equation out of the Langevin (2). In the Itô framework, this yields

$$\frac{\partial P(L, t)}{\partial t} = -\frac{\partial}{\partial L} \{c P(L, t)\} + \frac{1}{2} \frac{\partial^2}{\partial L^2} \{(\alpha^2 + \sigma^2 L^2) P(L, T)\}, \tag{4}$$

where $P(L, t)$ is the probability of having a certain liquidity value at time t . Assuming that there is a stationary solution, which means that $\partial P / \partial t = 0$, we get

$$\frac{d}{dL} [(\alpha^2 + \sigma^2 L^2) P] = 2c P + \kappa, \tag{5}$$

where κ is a constant. κ can take any value, but for convenience, we can take $\kappa = 0$ and check if a solution exists. In this case, it does exist, and it is

$$P(L) = \frac{c e^{\frac{2c \operatorname{Atan}((L-L_0)\sigma/\alpha)}{\alpha\sigma}}}{\sinh(\frac{c\pi}{\alpha\sigma}) (\alpha^2 + \sigma^2 (L - L_0)^2)}. \tag{6}$$

$\operatorname{Atan}()$ stands for the arctangent function, $\sinh()$ is the hyperbolic sine, and L_0 the initial liquidity. Note that the liquidity distribution shows a power-law decay for large values of L as $\sim L^{-2}$. The probability of default, P_b , can then be calculated by integrating $P(L)$ for the negative liquidity values, which yields

$$\begin{aligned} P_b &= \int_{-\infty}^0 P(L) dL \\ &= \frac{1}{2 \sinh(\frac{c\pi}{\alpha\sigma})} \left[e^{-\frac{2c \operatorname{Atan}(L_0\sigma/\alpha)}{\alpha\sigma}} - e^{-\frac{c\pi}{\alpha\sigma}} \right]. \end{aligned} \tag{7}$$

Given the relation between p and α , $\alpha = \sqrt{p(1 - p)}$.

It is interesting to repeat the calculation for $c = 0$. This can be done by retaking (5) and equating $c = 0$. The resulting stationary

distribution then becomes

$$P(L) = \frac{\alpha \sigma}{\pi (\alpha^2 + \sigma^2 (L - L_0)^2)}. \tag{8}$$

The probability of default is

$$P_b = \int_{-\infty}^0 P(L) dL = \frac{1}{2} - \frac{\operatorname{Atan}(L_0 \sigma / \alpha)}{\pi}. \tag{9}$$

This latter configuration provides a more symmetric solution with a Cauchy-Lorentz distribution. As occurs with the random walks and diffusion, the system shows memory effects since it remembers the initial condition with the distributions $P(L)$ remaining centered around L_0 . In contrast to diffusion, in this case, the distribution $P(L)$ reaches a stationary state. The role of the driving term c , which in the discrete model corresponds to the unbalance between money received and payments, is to induce an asymmetry in the liquidity distribution depending on the sign of c , and this is toward positive L if $c > 0$, and toward negative ones otherwise. The effect of c modulates thus (increases or decreases) the probability of bankruptcy.

The analytical results are confirmed by numerically integrating Eq. (2). Figure 1 shows the liquidity distributions obtained for several values of σ and c by direct Euler integration. $P(L)$ distributions are plotted when the system reaches a steady-state. The analytical expressions (6) and (8) represent the goodness of the analytical approximation fitting. One can easily appreciate how c introduces an asymmetry in $P(L)$. However, the interplay between the multiplicative noise σ and the driving c influences the bankruptcy probability [the integral of $P(L)$ for negative values of L].

IV. NUMERICAL SIMULATIONS ON DISCRETE EQUATIONS

To better understand the proposed model dynamics, we have built a single node network as depicted in Fig. 2(a). In this basic topology, a single node N_1 is connected to a market node N_0 , which provides it its earning and expenses.

As an initial experiment, we set the liquidity ratio R_s equal to 1, meaning that N_1 earns 0.1 from the market but pays 0.1 back to it. This R_s value means that N_1 trades without increases on average. We have simulated 10 000 different scenarios for 1000-time steps for several market noise values (σ) and activation of the system (p).

The starting liquidity of N_1 has been initialized at 0.1, being capable to do the first payment. However, if it is necessary, indebtedness is allowed. Hence, no Heaviside function is used in the model. This means that nodes are allowed to get into debt. With this setting in mind, we have simulated scenarios for economies with low volatility ($\sigma = 0.05$), medium volatility ($\sigma = 0.1$), and highly volatile economies ($\sigma = 0.3$). It is important to highlight that even if the σ parameter in both discrete and continuous models means the same, their values are not equivalent.

Intending to validate the discrete model, the distributions of the core system liquidity were also analyzed for different time steps. Figures 2(b)–2(d) show the liquidity distributions obtained for different values of σ and p . For time-step 1000, there is a peak around 0.1 and a symmetry: the distribution is symmetric as it is observed in the theoretical model when $c = 0$. The peak increases and tails

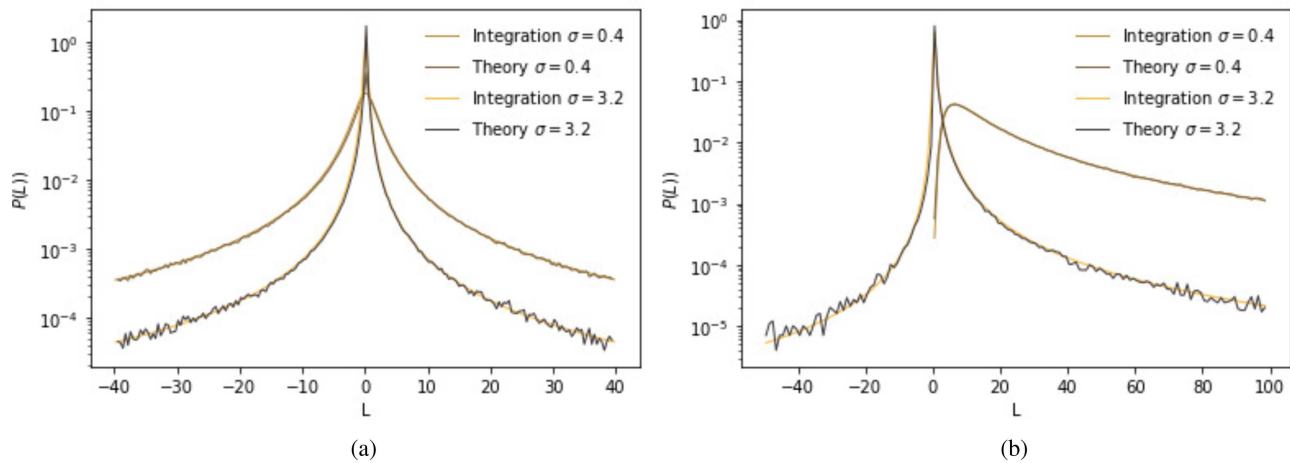


FIG. 1. Comparison of the distribution of liquidity for the continuous approximation integrating Eq. (2) and using the expressions (6) and (8). The integration is performed with an Euler method with $\Delta t = 0.01$, 1×10^6 noise realizations, and with initial liquidity $L_0 = 0.1$. In (a) without driving $c = 0$ and in (b) with $c = 1$.

flatten as volatility increases, although the distribution remains symmetric. However, the noise effect is still perceptible both in the peak but also in the tails of the distribution.

Another way of representing the distribution of the core system liquidity of N_1 is with boxplots. In Figs. 2(f)–2(h), the spread of the liquidity is greater for $p = 0.5$ and minimal for $p = 0$ and $p = 1$. This result is in line with the idea of maximum entropy systems, which reach their maximum variance where there is no information. This can be observed for any σ . Moreover, the median of the liquidity remains stable at 0.1, as expected since the liquidity ratio is 1. We also observe the effect of a higher peak and lower tails in the boxplots, with a smaller interquartile range.

This means that for a fully activated simulation ($p = 1$), N_1 earns 0.1 from N_0 and pays back 0.1. Therefore, in each time step, there are no profits. Similarly, for $p = 0$, N_1 neither pays anything nor receives money. Hence, its liquidity does not change because of the volatility of the market. For p between 0 and 1, we do observe a symmetric spread, which is consistent to what is observed in Figs. 2(b)–2(d). Depending on p , the spread of the liquidity for all possible scenarios increases until $p = 0.5$ when all possible cases (to pay–paid, to pay–not paid, not to pay–paid, not to pay–not paid) are equiprobable. For higher p , the spread decreases again.

Previous figures described the distribution of the liquidity; however, they are not very illustrative when we want to study if node

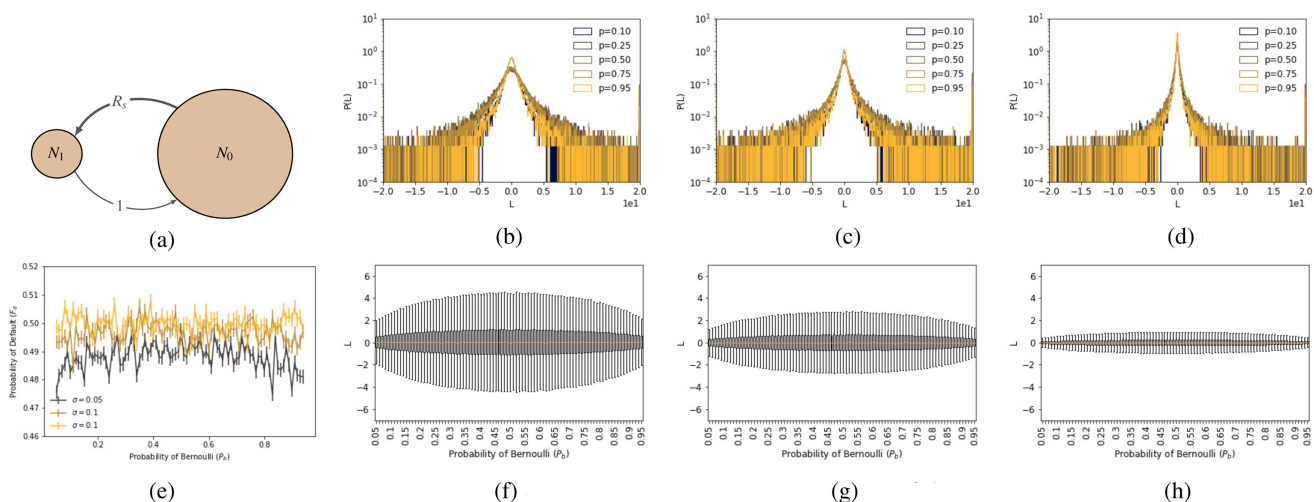


FIG. 2. (a) Topology of the one node network. (b)–(d) Distribution of the system liquidity at time $T = 1000$. Note that the y-scale is logarithmic. (e) Probability of default for one node. (f)–(h) Distribution of the system liquidity at time $T = 1000$.

N_1 is suffering from financial distress. To shed some light on this, we are going to assume that a node has financial distress when it has a negative liquidity value. We refer to these nodes as defaulted. This simplification allows us to introduce the idea of default probability as the probability that a node has negative liquidity. Figure 2(e) shows the behavior of such probability with respect to the Bernoulli probability for both simulations ($R_s = 1$).

The main result is that we observe a probability of default for any value of the Bernoulli probability. In the case of $R_s = 1$, the default probability tends to 0.5 as time increases. These two results mean that for any activation of the system, the distribution of liquidity tends to the perfect symmetry if $R_s = 1$. We also observe that the distribution of volatility σ does not influence this qualitative behavior of the probability of default concerning the Bernoulli probability.

V. NUMERICAL SIMULATIONS ON SYNTHETIC NETWORKS

To simulate the financial distress propagation on diverse substrates, we have extended our one node simulation to a more realistic setting. To implement that, there are two options: first, to simulate companies assuming we know all their connections, which is difficult to fulfill, and second, to create a market node that represents the unknown connections between companies and those with individuals. For this second option, we need to define an average liquidity ratio that companies must keep with the market node. For this case, the market node has infinite liquidity and transfers money to the nodes according to the liquidity ratio equal to 1.5.

To do so, we have created two power-law synthetic networks of 1000 nodes with and without market. In such networks, some nodes N_i are highly connected, meaning that they have many links to other

N_j nodes for $j \neq i$, although the number of connections among all nodes is low. Due to this, we replicate an economical structure with prevalent and secondary companies as it is observed in real markets.

We have generated both networks as follows: each new node adds three random edges, with a probability of adding a new triangle after adding an edge of 30%. In this case, we have a market node, and all nodes may be linked to the market node N_0 to keep a constant liquidity ratio.

To simulate a growing economic context, we set the liquidity ratio equal to 1.5. This means that for a fully activated simulation ($p = 1$), the single node earns 1.5 from the market node and pays back 1. Therefore, in each time step, profits are 0.5. For a lower activation of the system, benefits are lower. As in Sec. IV, the starting liquidity makes all nodes capable of withdrawing the first installment, indebtedness is allowed, and several scenarios are simulated for different volatilities of the market. For both substrates, we have calculated 1000 scenarios for 1000 time steps.

For a power law without the market, we observe that the distribution of liquidity is still symmetric as depicted in Figs. 3(b)–3(d). Moreover, we observe a similar behavior of the distribution of the liquidity as in the one node setting. That is for higher volatilities, the peak of the distribution increases (around 1.5 in this case), whereas the tails have a bigger spread. The boxplot for the highest probability of Bernoulli shows a greater spread of liquidity.

These new liquidity distributions are different because of the combination of the number of nodes and volatility. With 1000 nodes, the aggregated Bernoulli probability of all nodes acts as a binomial distribution, which occurs for both the earnings and payments. The spread of a binomial distribution increases with p , as it can be observed in Fig. 3(f)–3(h). We can confirm this for $\sigma = 0.05$ when the effect of volatility is very small. The spread of the liquidity is maximal for $p = 1$, whereas for $p = 0$, it is minimal. For higher

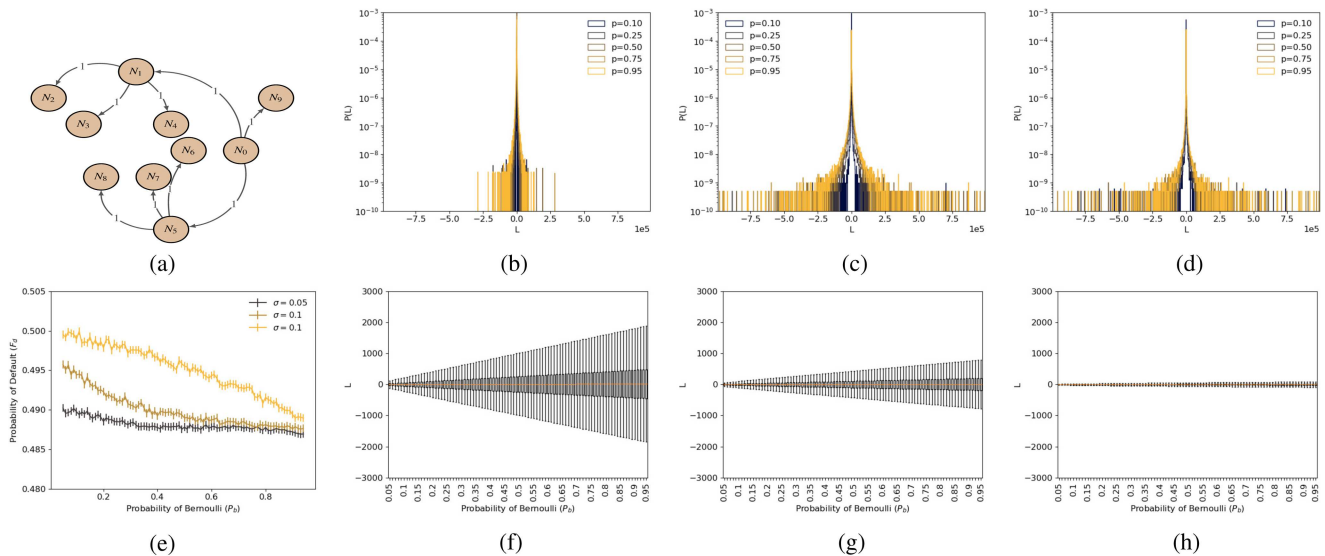


FIG. 3. (a) Topology of a power-law network without a market. (b)–(d) Distribution of the system liquidity at time $T = 1000$. Note that the y-scale is logarithmic. (e) Probability of default for a power-law network without a market. (f)–(h) Distribution of the system liquidity at time $T = 1000$.

volatilities, the multiplicative effect of σ shapes the distribution of the liquidity, with a maximum in $p = 0.5$. Therefore, we can conclude that the number of active edges matters concerning the range of the possible liquidity values.

Again, the probability of default [Fig. 3(e)] oscillates around 0.5 at time 1000 for any value of the Bernoulli probability. For this system, we have a liquidity ratio greater than 1, but there is no liquidity from the market. Note that this network acts at the end as a closed conservative system. The symmetry of the liquidity distribution is still present for any volatility. Nevertheless, we only detect little changes in spread depending on the activation of the network.

When analyzing the results of a network with market node N_0 , the main consequence of this addition is an asymmetry of the liquidity distribution and the consequent change of the default probability curve.

Figures 4(b)–4(d) represent the distribution of liquidity for a power-law network with the market. These graphs depict an asymmetry of the distribution of liquidity caused by the presence of the market node. The spreads are smaller due to the fewer number of edges between nodes in the power-law network. Both right and left tails flatten as higher is the σ , whereas the peak increases, as it was seen before.

The liquidity distribution asymmetry is clearly shown when we analyze the boxplot for this network [Figs. 4(f)–4(h)]. For any volatility, both the median and the spread increase with Bernoulli probability p . The increment of the median is caused indeed by the injection of credit by the market. On average, all nodes increase their cash flow every time step by 0.5. The median increase is lower as higher is the σ , and the distribution of liquidity becomes more symmetrical. The aggregated Bernoulli probability, which is a binomial distribution, causes a greater spread of liquidity.

This asymmetry affects the probability of default. In Fig. 4(e), the probability of being bankrupt decreases with the

activation of the system p . The cause of this exponential decrease of the probability of default vs p is that for a more active system, the market pays more money to the nodes; therefore, their capability of doing transactions increases. When observing different σ values, we note that the risk of default increases when σ increases. The reason for this increase is the larger instability of the market. This fact is coherent with the real economy, where the larger the uncertainty, the higher the risk of default.

In summary, the presence of a market node is crucial for the stability of the system. The fact that a market node always provides liquidity to the nodes causes an increase in the liquidity median. Contrarily, when there is no market node, the median of liquidity remains constant for any p . For the same reason, we cannot see any difference between the behavior for low and high volatility where there is a network without the market. Therefore, in that case, the liquidity ratio (R_s) and the Bernoulli probability [$P(t)$] control the risk of default.

VI. REAL CUSTOMER-SUPPLIER NETWORK EVALUATION

To confirm the validity of our model, we have studied the financial distress propagation in a real network. To do so, a static network was built using customer companies of a Spanish bank. Data cover relationships with both public and private Spanish firms. The construction's details of this real network are described in Appendix A.

Besides, we have also built a null model to understand the dependency of the results on the structural and dynamical properties of the system. To assess for structural dependencies of the results on the topology of the network and the weight distribution, we have generated a null model consisting of a synthetic generated Erdos–Renyi network with a similar number of nodes and edges as

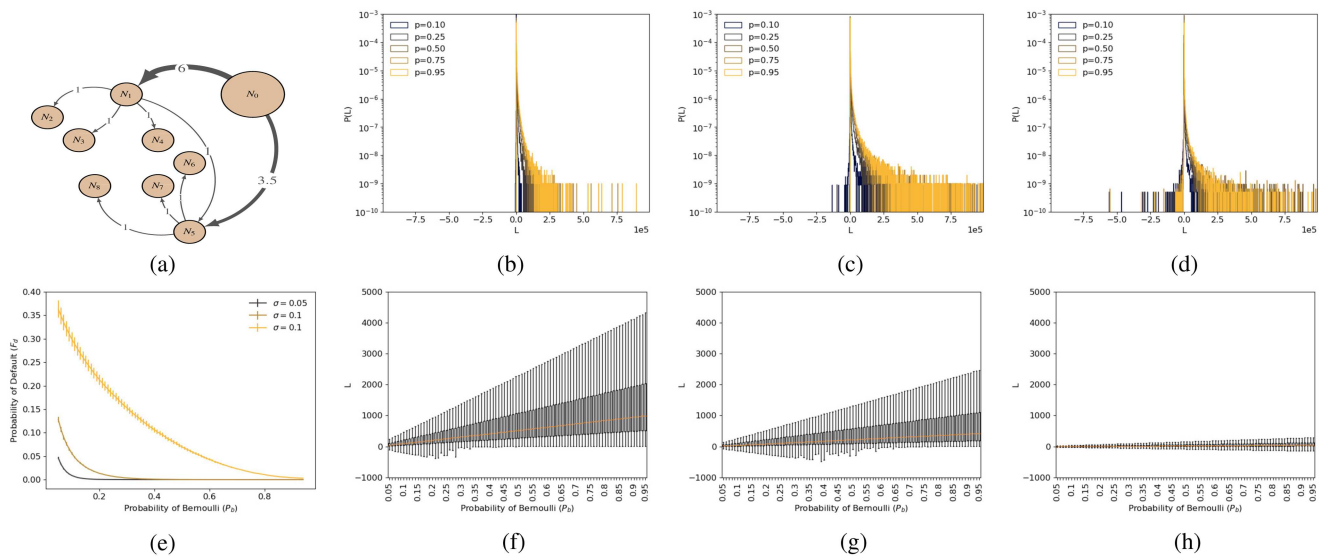


FIG. 4. (a) Topology of a power-law network with a market. (b)–(d) Distribution of the system liquidity at time $T = 1000$. Note that the y-scale is logarithmic. (e) Probability of default for a power-law network with a market. (f)–(h) Distribution of the system liquidity at time $T = 1000$.

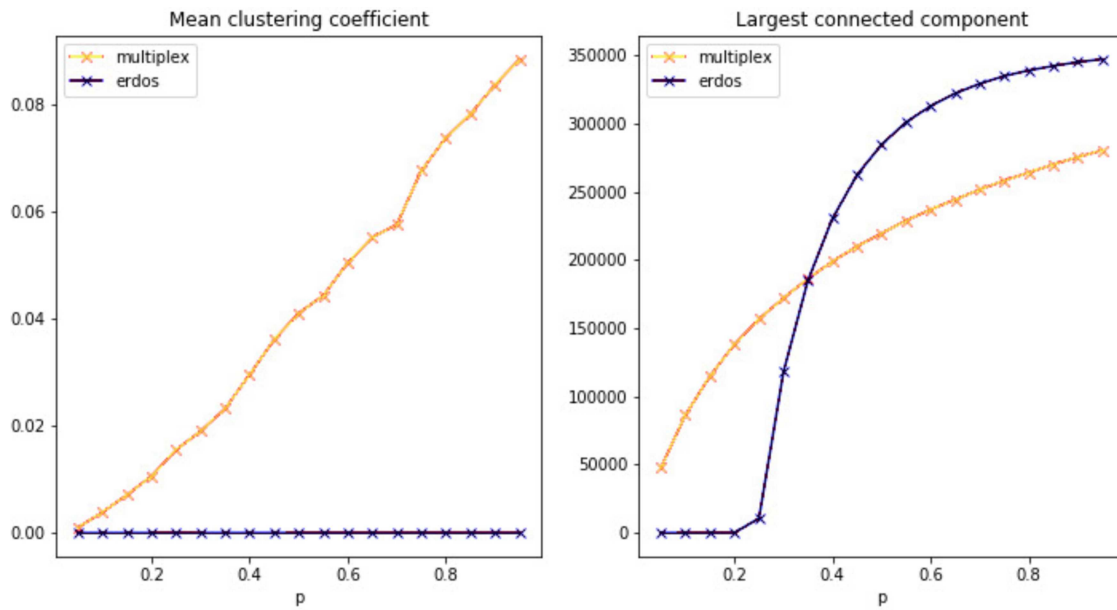


FIG. 5. Size of the largest connected component and the clustering coefficient for the Erdos–Renyi and the projected network as p varies.

the real network. The weight distribution is a Gaussian distribution of μ equal to 1000ϵ and σ equal to 100.

To compare both networks, Fig. 5 shows the size of the largest connected component and the clustering coefficient for the Erdos–Renyi and the projected network as p varies. We observe a typical percolation threshold in the case of the random network, while the increase of the size of the largest connected component

is more gradual for the case of the real network. The clustering coefficient is also larger for the real network.

Having this in mind, our goal here is to study the influence of the network structure on the fraction of defaulted companies. To do so, we have executed different simulations for several market volatility distributions and various values of active percentages of money exchanges within the network.

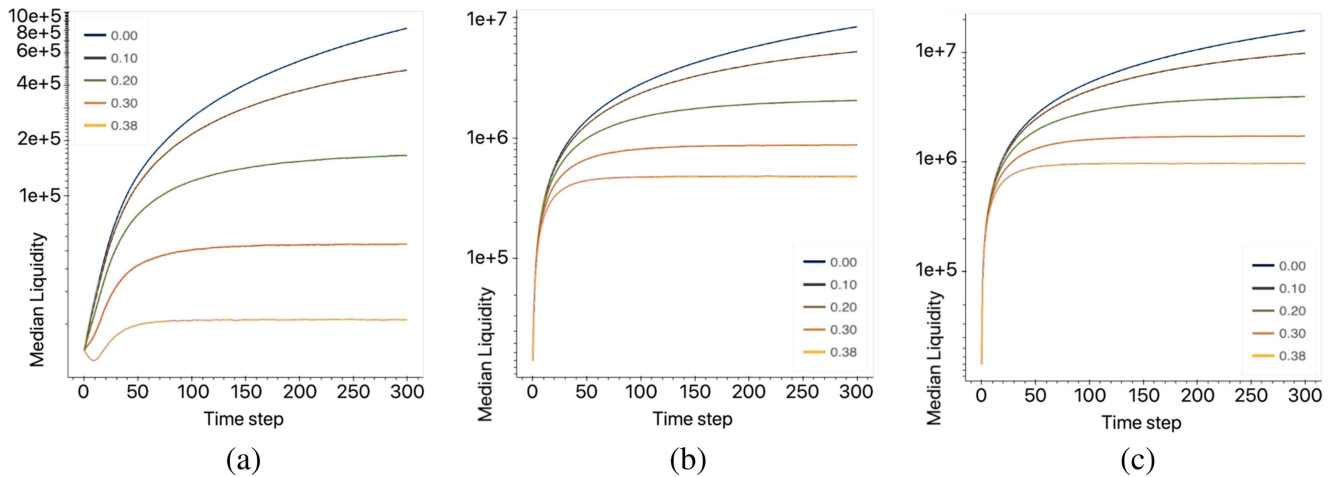


FIG. 6. Median of the core system liquidity at time T for different combinations of volatility σ and (a) low, (b) medium, and (c) large Bernoulli probability. On color, σ . Note that the y-scale is logarithmic and varies for the different subplots.

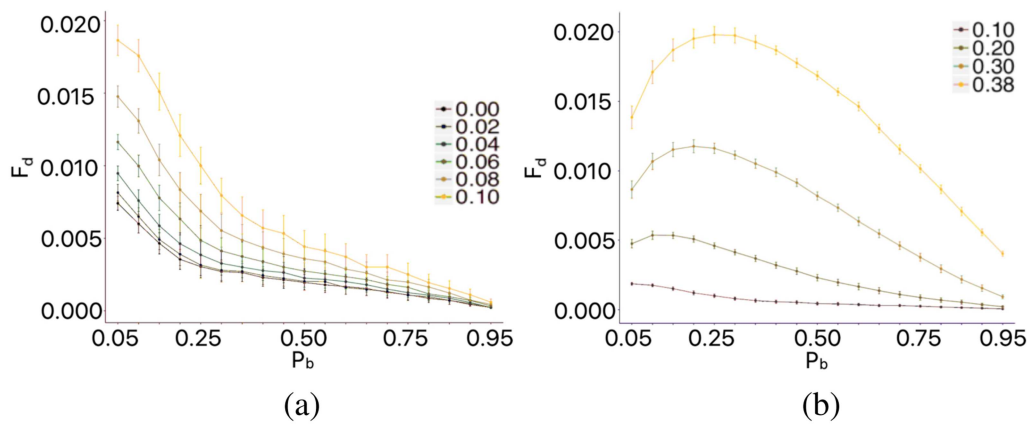


FIG. 7. Number of defaulted nodes as a function of Bernoulli probability (P_b) for (a) small and (b) large values of σ at time = 300 iterations.

In Fig. 6, the median of the network companies' liquidity reaches the steady-state for different combinations of the model parameters. We observe that for any activation p of the system, liquidity becomes steady for high volatility, whereas for simulations without volatility ($\sigma = 0$), liquidity is monotonically increasing.

Besides, Fig. 7 shows two different behaviors of the fraction of defaulted companies concerning the partial activation of payments of the real network. p^* is defined as the activation such that the system changes the state of activation. When a fraction of payments larger than p^* is activated ($p > p^*$), the global network is mainly active. As mentioned before, this may correspond to an economic situation reflecting times of economic wealth. According to the figure, increasing trade is always beneficial for the number of default nodes decreases. However, when a fraction of payments lower than p^* is activated ($p < p^*$), the effects of increasing trade depend on the distribution and magnitude of volatility. For low volatility or policies

that do not stray from normality, increasing trading is beneficial. However, for high volatility that may affect different companies in a different manner, increasing trade may allow instabilities in the network to propagate, increasing the number of default nodes.

To observe if this effect depends on the structure of the network, we compare the results to the ones obtained with the Erdos-Renyi null model. Figure 8 shows that the existence of a critical percentage of network activation p^* also occurs for the null model for high volatility, meaning that the network effect of instability propagation does not depend on the structural details of the network.

However, for low volatility, the qualitative response of the defaulted companies is very different for both networks. For the real network, there is a sharp decrease of the defaulted companies when the payments network starts to be activated (small p) and then decreases slowly, contrary to what happens for the Erdos-Renyi

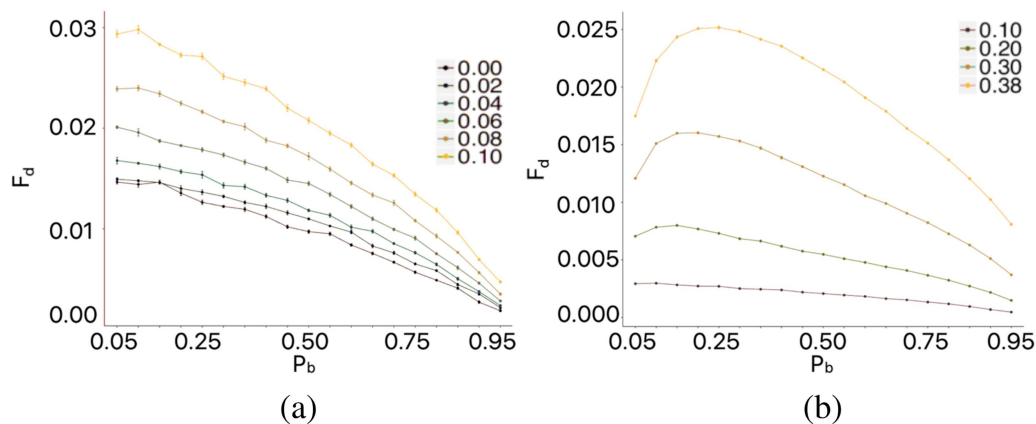


FIG. 8. Fraction of defaulted nodes (F_d) as a function of Bernoulli probability (P_b) for (a) small and (b) large values of σ at time = 300 iterations on the Erdos-Renyi synthetic network.

network. This behavior is directly linked to two variables: the different percolation thresholds and the different liquidity ratios at time 0 for the two networks. The real network does not show any percolation threshold as happens to the Erdos–Renyi. The largest connected component size increases progressively, and its larger slope occurs when the percentage of the network activation is lower than 20%. In this area, the network effect on the number of defaulted companies will be more pronounced [Fig. 7(a)]. Note that the liquidity ratio at time 0 also differs for the two networks, being larger for the real network (with a median of approximately 7) than for the Erdos–Renyi (with a median of approximately 1.7). These results in a sharper decrease of the fraction of defaulted nodes, as the network becomes activated, because nodes gain more from each interaction.

VII. CONCLUSIONS

In this article, we have presented a liquidity model to study how the risk of default propagates in economic networks. The networks represent economic transactions such as wires to pay for services or goods. The model is based on previous works on the wealth distribution and combining two stochastic terms: an additive noise, accounting by the capability of trading and paying obligations, and a multiplicative noise representing the variations of the market. The additive term is regulated by a parameter p . The larger the p , the more active, in terms of transactions, the network is. The multiplicative term is controlled by a parameter σ . In this case, market instability grows with large σ values. We solve analytically and numerically the model when the system is composed of a single agent and the environment (market). Our simulations show that network dynamics reach a steady-state even in the presence of large noise values. Besides, we also demonstrate that the probability of default in this steady regime reaches a maximum when the trading probability p is equal to 0.5. For a single agent network, the interplay between the outbalance of the initial income and outcome money flows and the multiplicative noise level σ leads to an asymmetry in the final liquidity distribution. Consequently, this affects the values of the default probability, even though its maximum still appears at $p = 1/2$. When many agents interact within a network, the maximum of the default probability displaces to other values of p . Moreover, when the network is heterogeneous enough in connectivity (e.g., scale-free), we observe cascades of default that may follow a power-law like distribution. Similar long-tailed cascades are obtained in real trading networks. To prove this, we have experimented with a network representing company–company interchange data collected by one of the main Spanish banks. From an economical perspective, it is important to note that one of the main effects of a crisis is to reduce trading. This means that the system moves to lower values of p , and, according to the model, the probability of default increases. This counter-intuitive result paves the way for theories that suggest that in an environment of increasing uncertainty, the deceleration of trading will worsen the crisis while encouraging trading will help to avoid default cascades.

Generally speaking, the particular network structure of the economic interaction network and the volatility σ are crucial to determining the maximum default probability. The shape of the default cascades is also determined by these two factors. The model

can thus help us to better understand the systemic risks of economic systems.

ACKNOWLEDGMENTS

We would like to thank Pere Colet and Raúl Toral for their useful inputs on stochastic equation treatment. A.A. acknowledges support by the Ministerio de Economía y Competitividad (Grant No. FIS2015-71582-C2-1), the Generalitat de Catalunya (Grant No. 2017SGR-896), the Universitat Rovira i Virgili (Grant No. 2017PFR-URV-B2-41), and the ICREA Academia and the James S. McDonnell Foundation (Grant No. 220020325). J.J.R. acknowledges funding from the Spanish Ministry of Science and Innovation, the AEI, and FEDER (EU) under the grant PACSS (No. RTI2018-093732-B-C22), and the Maria de Maeztu program for Units of Excellence in R&D (No. MDM-2017-0711).

APPENDIX A: REAL NETWORK CONSTRUCTION

To study financial distress propagation in a real network, we built a static network using BBVA customer companies. BBVA is the second-largest bank in Spain. Data cover relationships with both public and private Spanish firms. For each available company, we extracted several types of relationships described as follows and annually aggregate them over January to December 2016.

Concretely, we have used the following relationships provided by the BBVA data science team:

- *Customer–supplier third-party payment declaration.* Official customer–supplier relationships based on third-party payment declaration collected by the BBVA risk management department. This declaration is used as a mechanism to avoid fraud in companies' VAT declarations. In it, Spanish companies inform about their supplier payments and customer earnings.
- *Factoring/confirming financial products.* There are two types of edges including financial products relationship between firms: confirming and factoring. Confirming products are put up when a bank customer (firm) must pay its suppliers and signs a contract with the bank to be an intermediary in payments allowing the customer to stretch finance. Factoring products are put out by a bank customer (firm) having bills to charge their customers and signs a contract with the bank to be an intermediary and hedge their receipts, allowing the customer to anticipate payments.
- *Wire transfers.* Companies also make and receive payments via cash transfer.
- *Customs duties.* Companies also make and receive payments via customs duty.

The above-mentioned edges are directed and weighted according to the amount in euros transferred between companies. The direction of edges follows the path of money injection, e.g., from customer to supplier. All edges' weights are aggregated annually. Self-loops have been removed.

To avoid duplicating the data, if a customer–supplier third-party payment declaration edge exists, we remove any other edge between two companies for this edge includes all the others. If the edge does not exist, we sum the weight of the edges.

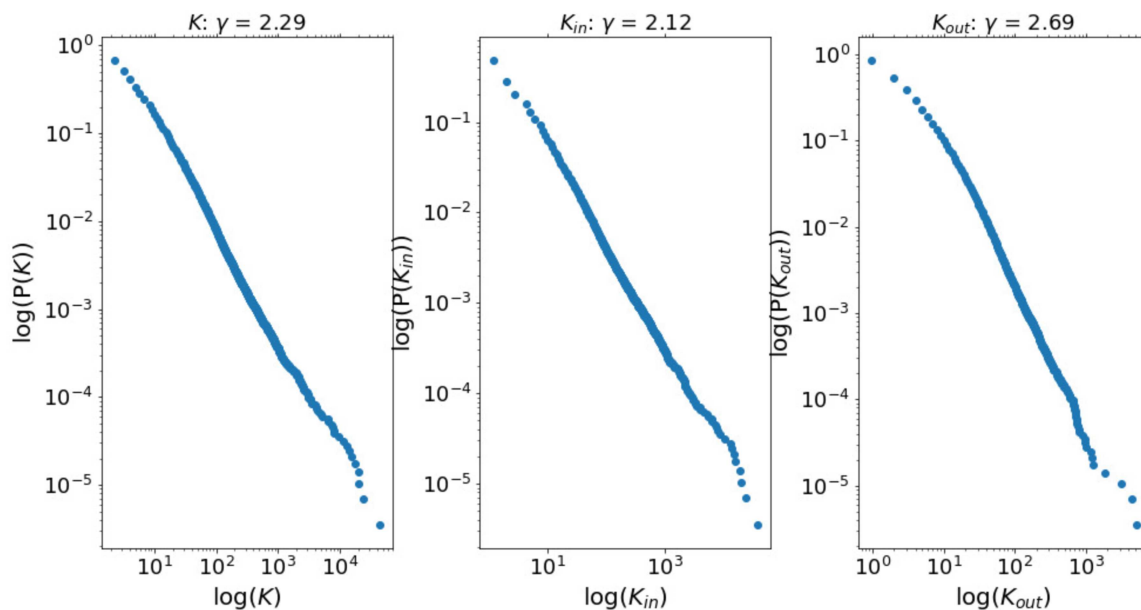


FIG. 9. Power law for the resulting real network.

Naturally, customers are also connected to other companies that are not BBVA customers and individuals. These types of entities are grouped on what we call the market node. The reason behind this decision is that the economical, financial, and connectivity information of BBVA non-client companies are incomplete, thus affecting the dynamics with missing information. Regarding individuals, these are considered to be part of the market because we are interested in modeling dynamics between companies. However, connections are left as edges (in and out) between BBVA customer companies and the market node because money flow between these entities is of paramount importance for their financial stress. Besides, originally, the number of BBVA customer companies in the raw data was 559 673, but 36.8% of companies, with a liquidity ratio different from zero, have negative liquidity every year. If these companies were incorporated into the network, they would originate a global failure in the dynamics. The reason for the negative liquidity is again missing information in most cases; therefore, we also group these companies as being part of the market node.

The resulting network is composed of 1 891 230 direct edges connecting 385 804 companies. As a result of this aggregation, the market node in-degree is 220 291, the out-degree 232 752, and its in-strength and out-strength in the order of billions and hundreds of billions, respectively. Figure 9 describes the power laws by degree, in-degree, and out-degree.

APPENDIX B: ERDOS-RENYI NULL MODEL

Finally, we can categorize companies regarding their connectivity. Consequently, we define “sink” companies as those who only have incoming edges. These are raw material suppliers where we

do not visualize their outgoing edges because most of them are too small natural resource producers and labor force. We categorize companies with in-and-out edges as “core” companies and are those companies that are in intermediate levels of the customer-supply chain. We are mostly interested in these because they can characterize their trade with close certainty. Besides, we encounter companies that have only outgoing edges (15.5% of the total share). These are mostly in the outermost level of the customer-supplier chain and are mainly retailers. We cannot leave out these because they are fundamental entities in the whole customer-supplier structure. Therefore, we create an incoming edge from the market node, thus resembling end-customer sales. The edge weight is 1.5 times their out-strength. The reason is that we do not want these to default because we cannot properly characterize their trade. In the end, we are only interested in the dynamics of the “core” nodes, and therefore, the results are focused on them.

To validate the results of the synthetic power-law networks described in Sec. V, we model an alternative monetary exchange with random edges among the nodes within an Erdos-Renyi network with and without a market. In these substrates, any node N_i is linked with the same probability to the other nodes, meaning that it is statistically independent of the rest of N_j nodes for $j \neq i$. All nodes are linked to the market node N_0 . Here, we first analyze the network without a market node and later including it.

In Figs. 10(b)–10(d), we observe a similar behavior of the distribution of the liquidity as in Sec. V. That is, for higher volatilities, the peak of the distribution increases (around 1.5 in this case), whereas the tails have a bigger spread. Despite this, the distributions depicted in Figs. 10(f)–10(h) show some differences compared to the power law’s charts. Here, for $\sigma = 0.05$, the maximum of liquidity spread is for the greatest activation of the system ($p = 1$).

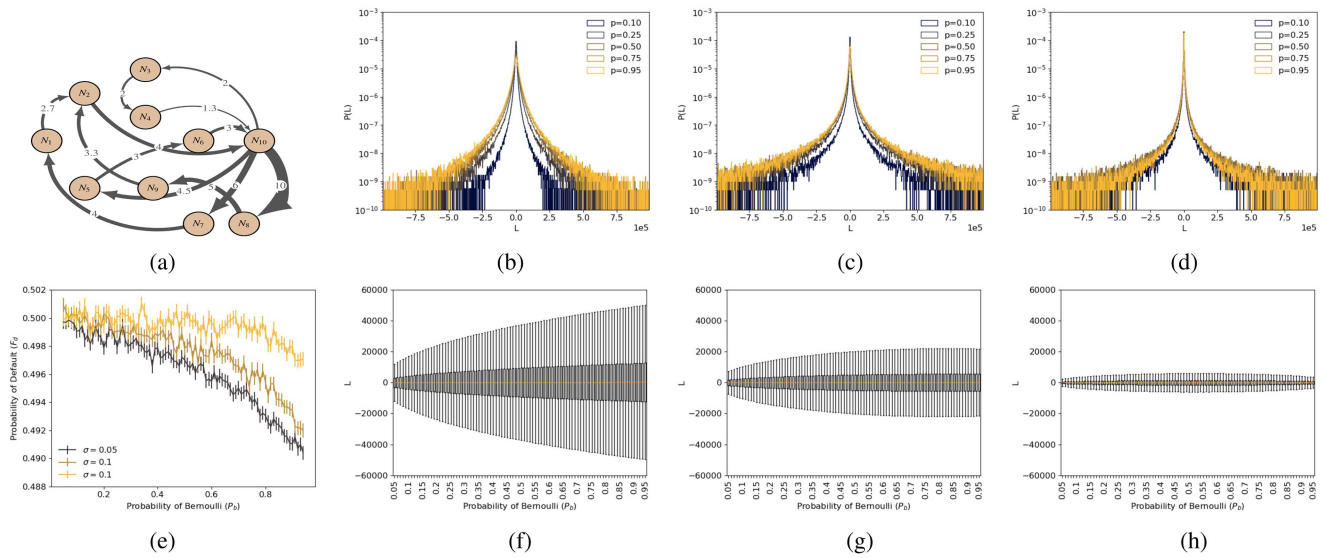


FIG. 10. (a) Topology of an Erdos–Renyi network without a market. (b)–(d) Distribution of the system liquidity at time $T = 1000$. Note that the y-scale is logarithmic. (e) Probability of default for an Erdos–Renyi network without a market. (f)–(h) Distribution of the system liquidity at time $T = 1000$.

Yet, for $\sigma = 0.1$, the maximum shifts to $p = 0.8$ and even to $p = 0.5$ for $\sigma = 0.3$.

Again, an Erdos–Renyi without a market acts as a closed conservative system. Therefore, the distribution of the liquidity tends to the symmetry for any volatility. However, the highest spread of liquidity does depend on the activation of the market.

For an Erdos–Renyi network with a market, we now observe a right-tailed liquidity distribution [Figs. 11(b)–11(d)]. This asymmetry is greater for larger Bernoulli probability p . However, differences between p become smaller when volatility increases. Both right and left tails flatten as higher is the σ , whereas the peak increases, as it was seen before. This asymmetry can also be observed in

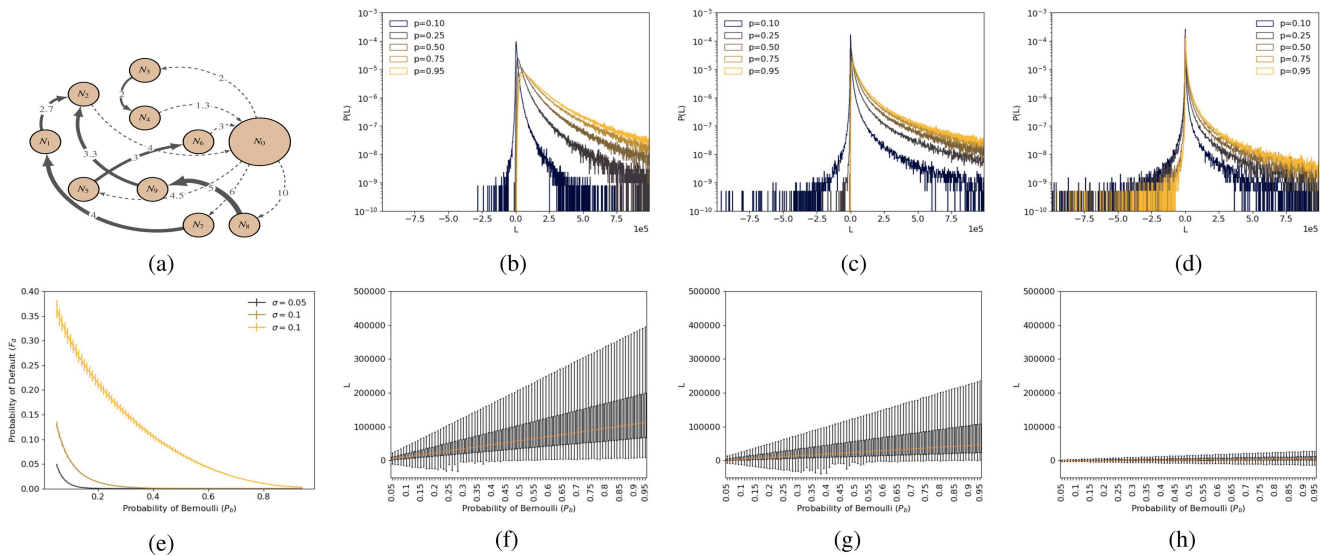


FIG. 11. (a) Topology of an Erdos–Renyi network with a market. (b)–(d) Distribution of the system liquidity at time $T = 1000$. Note that the y-scale is logarithmic. (e) Probability of default for an Erdos–Renyi network with a market. (f)–(h) Distribution of the system liquidity at time $T = 1000$.

Figs. 11(f)–11(h) and affects the probability of default. In Fig. 10(e), the probability of default also decreases with p .

We observe similar behavior of the probability of default for Erdos–Renyi and power-law networks. However, we detect a network effect between these two examples with and without a market. The connections of the nodes change, being the system more interconnected in the Erdos–Renyi than in the power-law network. The lower number of edges makes the power-law network less exposed to the volatility of the market than the Erdos–Renyi network.

DATA AVAILABILITY

Part of the data that support the findings of this study is available from BBVA. Restrictions apply to the availability of these data, which are used under license for this study. The data that support the findings of this study are available from the corresponding author upon reasonable request and with the permission of BBVA.

REFERENCES

- ¹M. Callon, *Sociol. Rev.* **38**, 132 (1990).
- ²D. M. Gale and S. Kariv, *Am. Econ. Rev.* **97**, 99 (2007).
- ³M. Timmer, E. Dietzenbacher, B. Los, R. Stehrer, and G. de Vries, *Rev. Int. Econ.* **23**, 575–605 (2015).
- ⁴A. Babus, *RAND J. Econ.* **47**, 239 (2016).
- ⁵A. Barja, A. Martínez, A. Arenas, P. Fleurquin, J. Nin, J. Ramasco, and E. Tomás, *EPJ Data Sci.* **8**, 32 (2019).
- ⁶F. Schweitzer, G. Fagiolo, D. Sornette, F. Vega-Redondo, A. Vespignani, and D. White, *Science* **325**, 422 (2009).
- ⁷A. H. AG and R. May, *Nature* **469**, 351–355 (2011).
- ⁸S. Battiston, M. Puliga, R. Kaushik, P. Tasca, and G. Caldarelli, *Sci. Rep.* **2**, 541 (2012).
- ⁹J. Nin and E. Tomás, “Default propagation in customer-supplier networks,” *J. Ambient Intell. Hum. Comput.* (published online 2019).
- ¹⁰M. A. Serrano and M. Boguñá, *Phys. Rev. E* **68**, 015101 (2003).
- ¹¹D. Garlaschelli, S. Battiston, M. Castri, V. D. Servedio, and G. Caldarelli, *Physica A* **350**, 491 (2005).
- ¹²M. O. Jackson and A. Watts, *J. Econ. Theory* **106**, 265 (2002).
- ¹³R. Coelho, Z. Neda, J. J. Ramasco, and M. A. Santos, *Physica A* **353**, 515 (2005).
- ¹⁴J.-P. Onnela, K. Kaski, and J. Kertész, *Eur. Phys. J. B* **38**, 353 (2004).
- ¹⁵M. Kosfeld, *Rev. Netw. Econ.* **3**, 20 (2004).
- ¹⁶J. Lorenz, S. Battiston, and F. Schweitzer, *Eur. Phys. J. B* **71**, 441 (2009).
- ¹⁷F. Caccioli, P. Barucca, and T. Kobayashi, *J. Comput. Soc. Sci.* **1**, 81–114 (2018).
- ¹⁸R. Burkholz, H. Herrmann, and F. Schweitzer, *Sci. Rep.* **8**, 6878 (2018).
- ¹⁹G. Caldarelli, S. Battiston, D. Garlaschelli, and M. Catanzaro, “Emergence of complexity in financial networks,” in *Complex Networks*, edited by E. Ben-Naim, H. Frauenfelder, and Z. Toroczkai (Springer, 2004), pp. 399–423.
- ²⁰Y. Leitner, *J. Finance* **60**, 2925 (2005).
- ²¹P. Gai and S. Kapadia, *Proc. R. Soc. London, Ser. A* **466**, 2401 (2010).
- ²²S. Battiston and G. Caldarelli, “J. Financ. Manage. Mark. Inst.” **2**, 129 (2013).
- ²³H. Watanabe, H. Takayasu, and M. Takayasu, *New J. Phys.* **14**, 043034 (2012).
- ²⁴H. Krichene, A. Chakraborty, H. Inoue, and Y. Fujiwara, *PLoS One* **12**, e0186467 (2017).
- ²⁵E. Letizia and F. Lillo, *EPJ Data Sci.* **8**, 21 (2019).
- ²⁶T. Roukny, H. Bersini, H. Pirotte, G. Caldarelli, and S. Battiston, *Sci. Rep.* **3**, 2759 (2013).
- ²⁷M. O. Jackson and A. van den Nouweland, *Games Econ. Behav.* **51**, 420 (2005).
- ²⁸H. Amini, R. Cont, and A. Minca, *Math. Finance* **26**, 329 (2013).
- ²⁹P. Glasserman and H. P. Young, *J. Bank. Finance* **50**, 383 (2015).
- ³⁰M. Bardoscia, S. Battiston, F. Caccioli, and G. Caldarelli, *Sci. Rep.* **8**, 14416 (2017).
- ³¹F. Corsi, F. Lillo, D. Pirino, and L. Trapine, *J. Financ. Stab.* **38**, 18 (2018).
- ³²K. J. Mizgier, S. M. Wagner, and J. A. Holyst, *Int. J. Prod. Econ.* **135**, 14–23 (2009).
- ³³P. Glasserman and H. Young, *J. Econ. Lit.* **54**, 779–831 (2016).
- ³⁴L. Veraart, *Math. Finance* **30**, 705 (2020).
- ³⁵J. Bouchaud and M. Mézard, *Physica A* **282**, 536–545 (2000).
- ³⁶C. Gardiner, *Stochastic Methods: A Handbook for the Natural and Social Sciences*, 4th ed. (Springer, Berlin, 2009).
- ³⁷R. Toral and P. Colet, *Stochastic Numerical Methods: An Introduction for Students and Scientists* (John Wiley & Sons, 2014).
- ³⁸G. Iori, S. Jafarey, and F. G. Padilla, *J. Econ. Behav. Organ.* **61**, 525 (2006).
- ³⁹G. Tedeschi, A. Mazloumian, M. Gallegati, and D. Helbing, *PLoS One* **7**, e52749 (2013).